Rev.Adv.Mater.Sci. 14(2007) 33-40

VANADOCHROMATES WITH DIVALENT METALS; STRUCTURAL AND MAGNETIC CHARACTERIZATION

A. Worsztynowicz[1], S. M. Kaczmarek[1], V. Mody[2] and R. S. Czernuszewicz[2]

[1]Institute of Physics, Szczecin University of Technology, Al. Piastów 48, 70-310 Szczecin, Poland
[2]Department of Chemistry, University of Houston, USA

Received: December 30, 2006

Abstract. Raman spectra of the $Mg_2CrV_3O_{11}$ and $Zn_2CrV_3O_{11}$ compounds were investigated and analyzed showing many similarities. X-ray diffraction studies of polycrystalline samples of $Zn_2CrV_3O_{11}$ and $Mg_2CrV_3O_{11}$ were performed. In case of $Mg_2CrV_3O_{11}$ we have obtained fairly good structure refinement. The symmetry of $Mg_2CrV_3O_{11}$ is triclinic space group P-1 with parameters: a = 0,6276(5) nm, b = 0,6705(2) nm, c = 1,123(2) nm, α = 113,9º, β = 106,4º, γ = 94,9º, Z = 2. It is isostructural with $Mg_xZn_{2-x}GaV_3O_{11}$. In $Mg_2CrV_3O_{11}$, the Cr^{3+} ion is distributed non-statistically with Mg^{2+} on two octahedral ($M(1)O_6$ and $M(2)O_6$) and one bipyramidal sites ($M(3)O_5$). Site-independent population refinements in the whole collected 2theta (8º-159º) range, and, correction made for the effect of finite sample size at the lowest angles, gave rise to the following distributions: M(1)=0.7Cr+0.3Mg, M(2)=0.24Cr+0.76Mg and M(3)=0.03Cr+0.97Mg. These distributions are different from those of Fe atoms in isostructural $Mg_2FeV_3O_{11}$ compound. Magnetic measurements were carried out for both compounds. The temperature dependence of the magnetic susceptibility of Cr^{3+}-Cr^{3+} dimers have been found using standard Van Vleck formula. The exchange constant J between Cr^{3+} ions has been successfully calculated taking also into account exchange interactions between dimers. Exchange constant between Cr^{3+} ions in dimer, J_1/k_B, calculated from magnetic susceptibility results, stay in good agreement with J calculated from EPR results.

1. INTRODUCTION

Multicomponent vanadates and their polymorphic modification attract particular interest due to their catalytic properties enabling their more and more comprehensive application in industrial practice as active and selective catalysts in many processes of oxidative dehydrogenation of lower alkanes [1]. Detailed understanding of catalytic properties of vanadates advocates searching for new vanadates, especially those with chains of face-sharing metal octahedra and isolated VO tetrahedra. Literature information implies that there exists a series of compounds of a general formula $M_2FeV_3O_{11}$ in the three-component metal oxide systems of MO–V_2O_5–Fe_2O_3 type where M = Mg, Zn, Ni [2,3]. The structures of $Zn_2FeV_3O_{11}$ and $Mg_2FeV_3O_{11}$ are known [3]. These compounds crystallize in the triclinic system and are isostructural with $Mg_xZn_{2-x}GaV_3O_{11}$ [4,5]. It is possible to find ternary vanadates with comparable structures by replacing the Fe in $M_2FeV_3O_{11}$ with chromium. Compounds of $M_2CrV_3O_{11}$ type being formed in the MO – V_2O_5 – Cr_2O_3 (M = Mg, Zn) systems have recently been obtained [6,7]. Their crystal structure

Corresponding author: A. Worsztynowicz, e-mail: adam.worsztynowicz@ps.pl

@ 2007 Advanced Study Center Co. Ltd.

is built of $M(1)O_6$ and $M(2)O_6$ octahedra, $M(3)O_5$ and $V(2)O_5$ trigonal bipyramids and two types of VO_4 tetrahedra. The chromium atoms are disordered between two or all three possible sites [M(1), M(2), and M(3)]. In the present paper, the structural properties of $M_2CrV_3O_{11}$ (M= Mg, Zn) powders and magnetic susceptibility measurements are presented.

2. EXPERIMENTAL

The following reagents were used in this research: V_2O_5, p.a. (Riedel-de Haën, Germany), Cr_2O_3, p.a. (Aldrich, Germany), $3MgCO_3{\cdot}Mg(OH)_2{\cdot}3H_2O$, p.a. (POCh, Gliwice, Poland). The reacting substances were weighed in appropriate portions, thoroughly homogenized by grinding, formed into pellets and heated in the air atmosphere in the following cycles: 450 °C (24 h) + 550 °C (24 h) + 700 °C (24 h) + 720 °C (24 h). After each heating cycle the samples were cooled to ambient temperature, ground and subjected to the XRD and DTA examination. Then they were again formed into pellets and heated, these procedures being repeated until samples in equilibrium state were obtained. Detailed description of synthesis, crystallographic findings, melting temperatures and the way of melting, also the infrared absorbtion (IR) investigations have been collected in [6,7].

Raman spectra were collected under the control of Spex DM3000 microcomputer system using a conventional scanning Raman instrument equipped with a Spex 1403 double monochromator (with a pair of 1800 grooves/mm gratings) and a Hamamatsu 928 photomultiplier detector. The spectra were obtained in solid state at room temperature using the front-scattering geometry (135° angle) with 514.5 nm excitation, 100 mW laser power, and 6 cm^{-1} slit widths. All samples were spun to avoid thermal decomposition. Sample pellets were prepared by mixing the compounds with dried anhydrous KCl.

The diffraction measurements were performed using a Bragg–Brentano diffractometer. The X-ray diffraction data were collected in a broad 2θ range (8^o – 150^o 2θ) using the Cu $K_{\alpha1}$ radiation. The monochromator cuts off the white radiation and the K_β component, as well as emission lines from anode-material impurities, while the contribution of Cu $K_{\alpha2}$ component is reduced to a negligible value. The chosen experimental setting is well suited for structural analysis, in particular, impurity phases at a very low level can be detected. And indeed, phase analysis indicates that there are no impurity phases in the $Mg_2CrV_3O_{11}$ samples, even as reagents phases are detected in powder pattern of $Zn_2CrV_3O_{11}$. The data were recorded with the 0.017° (2θ) step. The data collection time was 24 h. The correctness of the zero-position was verified through refinement of data of an external Al_2O_3 standard. The experimental data conditions of the collection are summarized in Table 1. More detailed description of the structure of investigated samples is presented in [8] while applied-instrument setting in [9].

Magnetic measurements were carried out using a MPMS-5 SQUID magnetometer. Zero-field-cooled (ZFC) and field-cooled (FC) magnetization measurements were made in the temperature range 2-300K at constant magnetic field. The isothermal magnetization was measured versus temperature and magnetic field up to 50 kOe.

3. RESULTS AND DISSCUSION

3.1. Raman spectroscopy

In Figs. 1-2 one can see Raman spectra of $Zn_2CrV_3O_{11}$ and $Mg_2CrV_3O_{11}$ compounds, respectively, in 100-1100 cm^{-1} range. The low frequency spectra below 700 cm^{-1} region, are richly populated with weak Raman bands, most likely arising from metal–oxo deformation and crystal lattice vibra-

Table 1. Experimental setting used for data collection.

Radiation	Cu $K_{\alpha1}$ (40 kV, 35 mA)
Wavelength [Å]	1.54060
Monochromator	Johansson (Ge) at the incident beam
Diffractometer radius	240 mm
Divergence slit	1°
Soller slits	At the incident and diffracted beam
Detector	Strip detector with full opening (127 strips, 9 mm active length corresponding to 2.1° 2θ)
Angular range	Detected 8-150° 2θ, refined 8-80° 2θ
Scanning mode	Continuous scanning mode, data recorded with the step 0.017° 2θ
Total scanning time	24 h

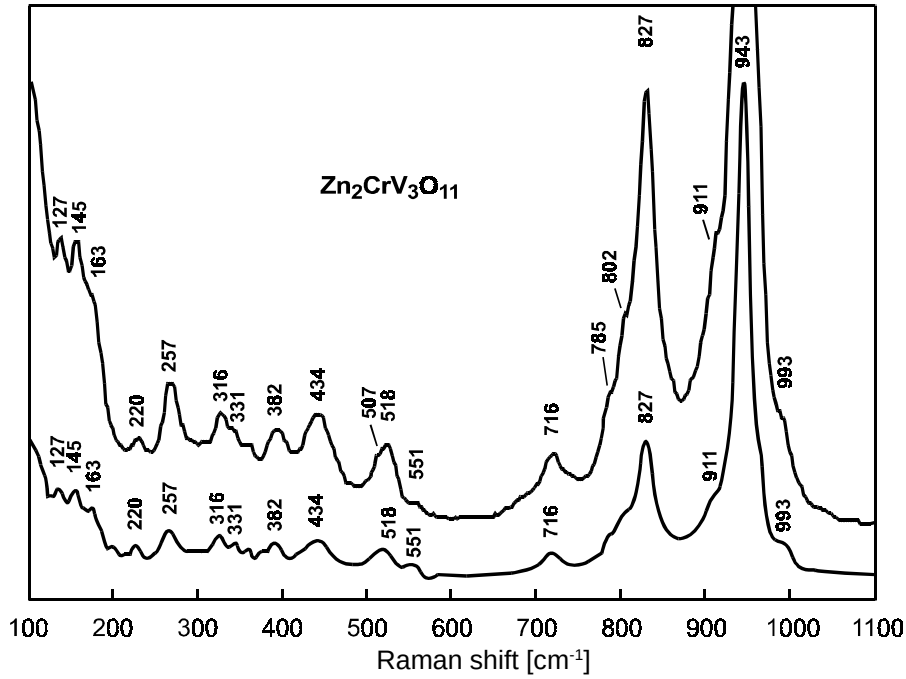

Fig. 1. Raman spectra of $Zn_2CrV_3O_{11}$ compound.

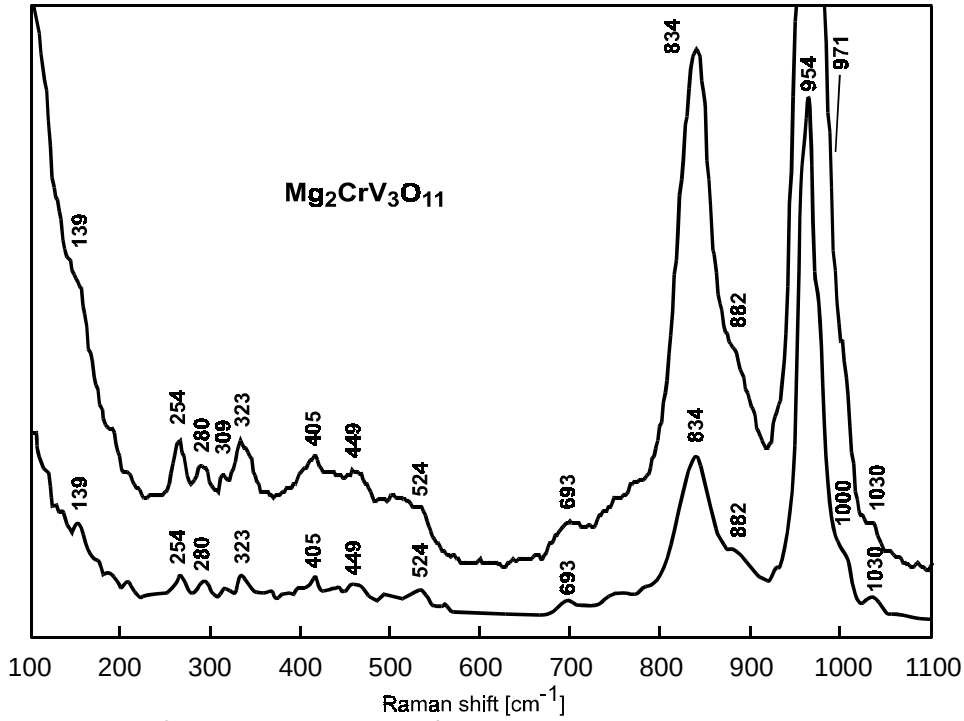

Fig. 2. Raman spectra of $Mg_2CrV_3O_{11}$ compound.

tional modes. Each compound shows its own vibrational pattern in the 100–700 cm^{-1} region, but both $Zn_2CrV_3O_{11}$ and $Mg_2CrV_3O_{11}$ compounds are very similar in appearance. So, these compounds seem to be very close analogs.

The mid-frequency spectra above 700 cm^{-1} show the most prominent differences in Raman bands among the two compounds. This region contains metal–oxo stretching vibrations. The intense bands above 900 cm^{-1} are assigned to vanadium-oxo stretch, ν(VO). The ν(VO) stretch occurs as a single and sharp band at 943 and 959 cm^{-1} for Zn and Mg analogs, respectively. The 943 cm^{-1} band of $Zn_2CrV_3O_{11}$ has weak shoulders at ~911,

~963, and 993 cm^{-1}. The magnesium analog has strong shoulders on both sides of the 959 cm^{-1} band at ~954 and ~971 cm^{-1}, as well as an additional weak shoulder at ~1000 cm^{-1}.

In the Raman spectra of the zinc and magnesium analogs we see, moreover, single and broad bands centered near 827 and 834 cm^{-1}, respectively. The 827 and 834 cm^{-1} bands can be assigned to the ν(ZnO) and ν(MgO) stretches, respectively, with the n(CrO) modes of these two compounds being shifted up in frequency into the ν(VO) region above 900 cm^{-1}.

3.2. Crystal structure

Structure refinement was carried out using the Full-Prof program [10] based on the multi-phase Rietveld analysis method. Rietveld-refinements were made using the collected data over 8°-159° 2θ angle range. Due to complicated background shapes the actual background has been calculated from the read one applying the formula with four coefficients given in Full-Prof manual. Correction for the effect of finite sample size at the lowest angles was taken also into account.

Probably, due to the presence of impurity reagents phases in powder pattern (Fig. 3a), the structure Rietveld refinement of $Zn_2CrV_3O_{11}$ has not been performed with satisfactory results. Phase analysis performed for the compound has shown that reagents are present in the compound only in the amount of 0.3% and are known. For magnetic susceptibility measurements the amount is not sufficient, while for EPR measurements it seems enough to show discrepancies in the EPR spectra.

The refinement of $Mg_2CrV_3O_{11}$ crystal structure has been successfully done (Fig 3b). A summary of crystallographic data is provided in Table 2, while atomic parameters and detailed structure description for $Mg_2CrV_3O_{11}$ is presented in [8].

The powder X-ray structural determination of $Mg_2CrV_3O_{11}$ showed that this compound is isostructural with $Mg_xZn_{2-x}GaV_3O_{11}$ [4,5]. The magnesium and chromium atoms are distributed non-statistically between three different crystallographic sites: M(1) and M(2) with octahedral coordination and M(3) with trigonal bipyramidal coordination (Fig. 4). Vanadium V^{5+} sites are in edge-connected trigonal bipyramids forming $V_4O^{8-}_{14}$ cluster and isolated VO_4 tetrahedron. As one can see in Fig. 5 each $M(3)O_5$ bipyramid shares an edge with one $M(2)O_6$ octahedron and a corner with one $M(1)_2O_{10}$ octahedral dimer.

Table 2. The values of crystallographic parameters.

Chemical formula	$Mg_2CrV_3O_{11}$
Formula weight	429.43
Space group	P-1
Initial cell volume (nm)	410.8712
a (Å)	6.4055
b (Å)	6.8109
c (Å)	10.0637
α (deg)	97.522
β (deg)	103.351
γ (deg)	101.750
Z	2
ρ_{calc} ($g \cdot cm^{-3}$)	3.50
R^a	1.6810
R_b^b	10.84
R_w^c	2.2969

$$^{a}R = \frac{\sum \left| |F_0| - |F_C| \right|}{\sum |F_0|},$$

$$^{b}R_b = \frac{\sum \left| |F_0| - |F_C| \right|}{\sum \left| |F_0| - |B| \right|},$$

$$^{c}R_w \sqrt{\frac{w \sum \left| |F_0| - |F_C| \right|^2}{\sum w |F_0|^2}},$$

$$w = \frac{1}{\sigma^2} F_0$$

Room temperature Rietveld structure refinements were performed taking the triclinic $Mg_2FeV_3O_{11}$ crystal structure as starting model. The distribution of the Mg and Cr atoms was established by examining the results of least-squares refinements.

Site-independent population refinements gave rise to the following distributions: M(1)=0.7Cr+ 0.3Mg, M(2)=0.24Cr+0.76Mg and M(3)=0.03Cr+ 0.97Mg, while the expected stoichiometric one is 1:2. The total atomic ratio Cr to Mg was not constrained and the population of disordered atoms was not fixed. So, M(1) position is substituted mainly by Cr ions while M(3) position is substituted only by Mg ions.

3.3. Static magnetization

Figs. 6 and 7 show the temperature dependence of inverse magnetic susceptibility χ^{-1} and effective

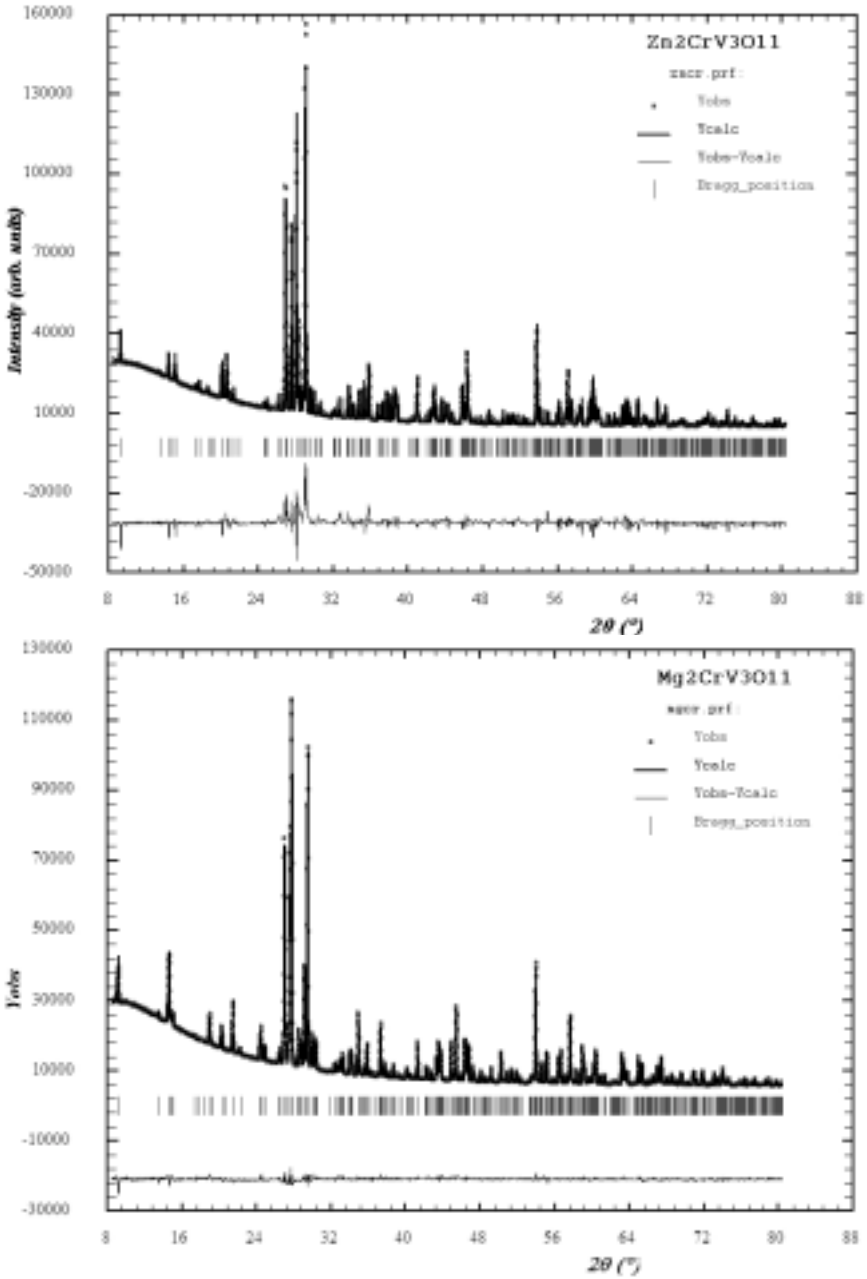

Fig. 3. Rietveld refinement result for the a) $Zn_2CrV_3O_{11}$ and b) $Mg_2CrV_3O_{11}$ powders, experimental – dotts, calculated – solid line. The difference pattern is shown below the powder pattern.

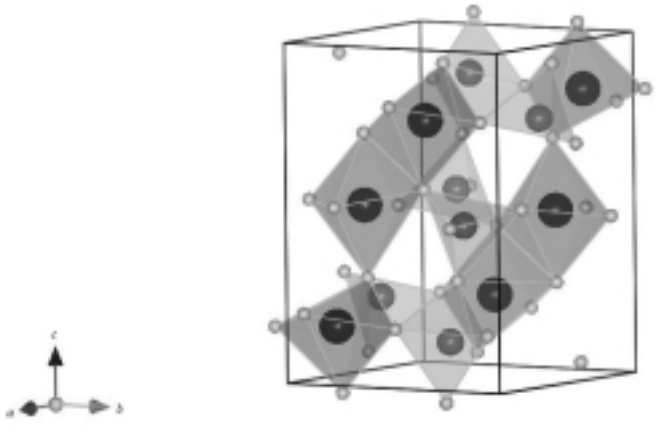

Fig. 4. Structure of the $Mg_2CrV_3O_{11}$ compound. Larger circles – Cr, Mg; middle circles – V, lower circles – O. Cr and Mg enter M(1), M(2) octahedra and M(3) trigonal bipyramid, V enter tetraheders and trigonal bipyramids.

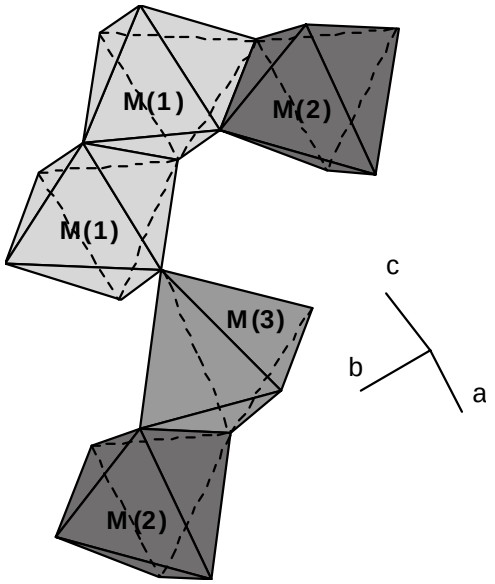

Fig. 5. The linkage among $M(1)O_6$, $M(2)O_6$ octahedra and $M(3)O_5$ trigonal bipyramid.

magnetic moment μ_{eff} for all the investigated samples. The value of χ^{-1} has been derived from static magnetization measurements in the ZFC mode as M_{ZFC}/H. There was no difference between the susceptibility measured under FC and ZFC conditions. The magnetic susceptibility exhibits a weak maximum within low fields with significant field dependence at Neal temperature, T_N=11K and T_N=10K for $(Zn, Mg)_2CrV_3O_{11}$, respectively. Below these temperatures it increases slightly as $T \rightarrow 0$. Typical antiferromagnetic behavior is decrease of the magnetic susceptibility towards zero as temperature approaches 0K. The behavior of χ^{-1} is almost linear at high temperature region. The effective magnetic moment at high temperature is equal to 3.5 μ_B which make ~90% of spin-only value, 3.88 μ_B, for Cr^{3+} ions.

The magnetic susceptibility of $Zn_2CrV_3O_{11}$ and $Mg_2CrV_3O_{11}$ has been calculated using the standard formula for two linearly coupled S=3/2 spins of Cr^{3+} ions in dimer, which result from the isotropic spin-coupling Hamiltonian in an external magnetic field H along z direction [11]

$$H = -2J_1 s_1 s_2 - g\mu_B HS - 2J_2 S_Z < S_Z >, \qquad (1)$$

where J_1 is the intradimer exchange integral for Cr^{3+}-Cr^{3+} interaction and J_2 denotes the interdimer exchange interaction between Cr^{3+}-Cr^{3+} dimers. Magnetic susceptibility of metal Cr^{3+} dimers has been found using standard Van Vleck formula [12],

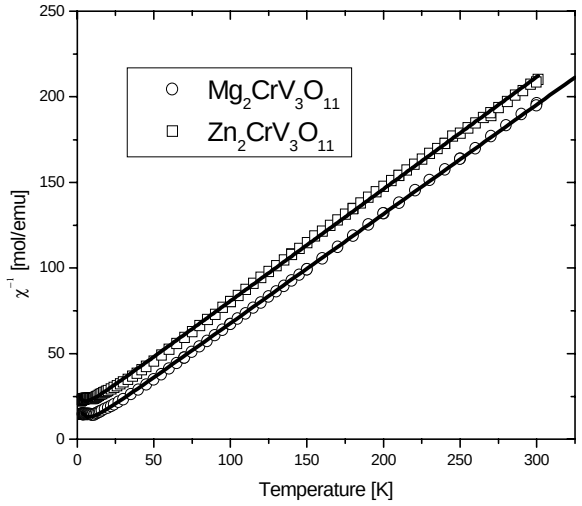

Fig. 6. Inverse magnetic susceptibility χ^{-1} versus temperature for $Zn_2CrV_3O_{11}$ (squares) and $Mg_2CrV_3O_{11}$ (circles) compounds.

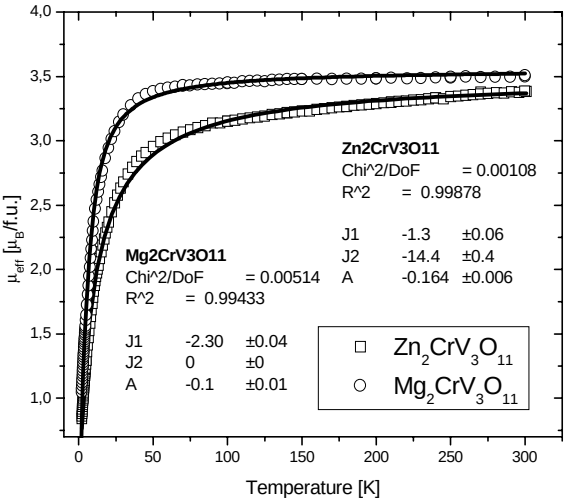

Fig. 7. The effective magnetic moment μ_{eff} vs. temperature for $Zn_2CrV_3O_{11}$ (squares) and $Mg_2CrV_3O_{11}$ (circles) samples.

as a mean of the susceptibilities of the individual spin levels, each of them being weighted by its degeneracy.

The corresponding results for Cr^{3+}-Cr^{3+} (S_{Cr}=3/2) dimers can be expressed by:

$$\chi(T) = \frac{N_A g^2 \mu_B}{3k_B} \frac{F(J_1,T)}{kT - 2J_2 F(J_1,T)} + \frac{A}{T}, \qquad (2)$$

where:

$$F(J_1,T) = 2\frac{\exp\left(\frac{2J_1}{T}\right)+5\exp\left(\frac{6J_1}{T}\right)+14\exp\left(\frac{12J_1}{T}\right)}{1+3\exp\left(\frac{2J_1}{T}\right)+5\exp\left(\frac{6J_1}{T}\right)+7\exp\left(\frac{12J_1}{T}\right)} \quad (3)$$

Other notations are those commonly used. The experimental values of c have been fitted to above equation by treating J_1 and J_2 as adjustable parameters. The resulting fitting of the effective magnetic moment μ_{eff} is shown as solid lines in Figs. 6 and 7, for which J parameters are: J_1/k = -1.30(6)K, J_2/k = -14.4(4)K and J_1/k = -2.30(4)K, J_2/k = 0K for $Zn_2CrV_3O_{11}$ and $Mg_2CrV_3O_{11}$ respectively. The order of the intradimer exchange interaction constant, J_1, stay in good agreement with exchange interaction constant found from EPR results [13].

As one can see, the value of interdimer exchange interaction parameter, J_2/k, for $Zn_2CrV_3O_{11}$ is too high. The theory of weakly interacting dimers is valid in the approach when the intra-cluster exchange J_1 is much more than inter-cluster exchange J_2. We have checked the value many times and each time it was too high for $Zn_2CrV_3O_{11}$ compound in the same way. Based on the Rietveld refinement results of $Mg_2CrV_3O_{11}$, which is isostructural to $Zn_2CrV_3O_{11}$, we think that larger distance (~6.5 Å) between Cr(2) and Cr(3) in dimer than the distance (~5 Å) between dimers can cause probably such differences in the exchange constants J_1/k = - 1.30(6)K and J_2/k = -14.4(4) for $Zn_2CrV_3O_{11}$. Moreover, we do not know up to now which is the distribution of Cr and Zn ions between M(1), M(2), and M(3) positions in the compound. The distributions of Cr and Mg ions between M(1), M(2), and M(3) positions presented in section 3.2 for $Mg_2CrV_3O_{11}$ suggest significant ordering at metal positions. In this case the distance between Cr ions is only 3.1 Å. So, this may be a reason why interdimer exchange interactions in a cluster vanish in case of $Mg_2CrV_3O_{11}$ compound.

The above discussion suggests the necessity of taking into account of some type of cluster model to explain the problem at all.

4. CONCLUSIONS

Raman spectra have shown each of $Zn_2CrV_3O_{11}$ and $Mg_2CrV_3O_{11}$ compounds shows its own vibrational pattern in the 100–1100 cm^{-1} region, but both compounds are very similar in appearance.

X-ray diffraction studies of polycrystalline samples of $Zn_2CrV_3O_{11}$ and $Mg_2CrV_3O_{11}$ reveal that they are isostructural with $Mg_xZn_{2-x}GaV_3O_{11}$. The Cr^{3+} and Mg^{2+} ions are found to be disordered in their corresponding structures, and their distributions on the octahedral and trigonal bipyramidal sites are non-statistical. Site-independent population refinements gave rise to the following distributions: M(1)=0.7Cr+0.3Mg, M(2)=0.24Cr+0.76Mg and M(3)=0.03Cr+0.97Mg.

Magnetic susceptibility on the recently synthesised vanadates $M_2CrV_3O_{11}$ (M = Zn, Mg) provide experimental evidence that Cr^{3+} ions in the compounds form clusters, may be pairs. The exchange constant, J, calculated using equation (2) was equal to: J_1/k = -1.30(6)K, J_2/k = -14.4(4)K and J_1/k = -2.30(4)K, J_2/k = 0K for $Zn_2CrV_3O_{11}$ and $Mg_2CrV_3O_{11}$ respectively. The sign of J is negative and indicates antiferromagnetic interactions. Different Cr-Cr distances between the compounds can cause different value of J constant inside dimer and between different dimers. In case of $Mg_2CrV_3O_{11}$ there are not present interdimer exchange interactions. Antiferromagnetic coupling between different dimers in $Zn_2CrV_3O_{11}$ result probably from higher ordering in substitution of M(1) and M(2) sites for Cr^{3+} ions. To be sure of the conclusion it is necessary to perform Rietveld refinement investigations of $Zn_2CrV_3O_{11}$. In the fitting procedure of the effective magnetic moment we took into consideration magnetic susceptibility arising from Cr^{3+} dimers [11]. Results of the fitting parameter of exchange constant, J, qualitatively agree with EPR measurements [13]. At high temperature range, results of the fitting agree very well with the experimental data for all the samples and could be effectively reduced to the Curie law. This also stays in agreement with the EPR measurements, in which only one EPR line is clearly observed at high temperatures.

ACKNOWLEDGEMENTS

The authors deeply acknowledge to Professor Jolanta Kurzawa from the Department of Inorganic and Analytical Chemistry, Szczecin University of Technology, Poland for powder preparations and Professor Ritta Szymczak from the Institute of Physics Polish Academy of Sciences, Warsaw, Poland for susceptibility measurements. This work was partially supported by the grant No. 11-072-0120/17-88-00 (to S.M.K.) and by the Robert A. Welch Foundation (grant E-1184 to R.S.C.).

REFERENCES

[1] P. Rybarczyk, H. Berndt, J. Radnik, M. Pohl, O. Buyevskaya, M. Baerns and A. Bruckner // *J. Catal.* **202** (2001) 45.
[2] I.Rychlowska-Himmel and A.Blonska-Tabero // *J. Therm. Anal. Cal.* **56** (1999) 205.
[3] X.Wang, D.A.Vander Griend, Ch.L.Stern and K.R.Poeppelmeier // *J. Alloys Comp.* **298** (2000) 119.
[4] C.Müller and H.Müller-Buschbaum // *J. Alloys Compd.* **191** (1993) 251.
[5] C.Müller and H.Müller-Buschbaum // *J. Alloys Compd.* **185** (1992) 163.
[6] M. Kurzawa, I. Rychlowska–Himmel, A. Blonska–Tabero, M. Bosacka and G. Dabrowska // *Solid State Phenom.* **90-91** (2003) 353.
[7] M. Kurzawa and M. Bosacka // *Solid State Phenom.* **90-91** (2003) 347.
[8] A. Worsztynowicz, S. M. Kaczmarek, W. Paszkowicz and R. Minikayev, in press.
[9] W. Paszkowicz // *Nucl. Instrum. Meth. A* **551** (2005) 162.
[10] J. Rodriguez-Carvajal // *Physica B* **55** (1993) 192.
[11] R.L. Carlin, *Magnetochemistry* (Springer-Verlag, Berlin, 1986).
[12] J. H. Van Vleck, *The Theory of Electric and Magnetic Susceptibilities* (Oxford, UK, 1932).
[13] A. Worsztynowicz, S.M. Kaczmarek, M. Kurzawa and M. Bosacka // *J. Solid State Chem*. **178** (2005) 2231.